SAND99-0093 C

FLUID DYNAMICS IN SUCKER ROD PUMPS

by
Robert P. Cutler and A.J. (Chip) Mansure
Sandia National Laboratories
Albuquerque, New Mexico

Abstract

Sucker rod pumps are installed in approximately 90% of all oil wells in the U.S. Although they have been widely used for decades, there are many issues regarding the fluid dynamics of the pump that have not been fully investigated. A project was conducted at Sandia National Laboratories to develop an improved understanding of the fluid dynamics inside a sucker rod pump. A mathematical flow model was developed to predict pressures in any pump component or an entire pump under single-phase fluid and pumping conditions. Laboratory flow tests were conducted on instrumented individual pump components and on a complete pump to verify and refine the model. The mathematical model was then converted to a Visual Basic program to allow easy input of fluid, geometry and pump parameters and to generate output plots. Examples of issues affecting pump performance investigated with the model include the effects of viscosity, surface roughness, valve design details, plunger and valve pressure differentials, and pumping rate.

Introduction

Many persistent problems in sucker rod pumping, including partial pump filling, gas interference, fluid pound, and compression loading of the valve rod are strongly influenced by the hydraulics of the pump. In rod string design and diagnostic programs these pump hydraulics effects are often lumped into 'pump friction factors' together with other effects such as friction between the rods and tubing. Pump friction consists of resistance to the plunger's downward movement due to hydraulic resistance of fluid flowing through the pump's internal passages, fluid resistance in the thin annulus between the plunger and the barrel, and any metal to metal sliding friction. This pump friction is often treated as a constant due to lack of an adequate model. The purpose of this project was to develop a general fluid model of downhole sucker rod pumps, which could predict for any given pump geometry, stroke rate, and well fluid properties the resulting flow rates and pressure drops anywhere in the pump throughout the stroke. A general fluid model would provide a better quantitative understanding of 'pump friction', allowing tradeoff studies of pump selection and stroke rate for a given well.

Some applications for such a model include:

1. To predict the differential pressure on the plunger as a function of fluid viscosity and pump stroke rate. This differential pressure contributes to the compressive load on the bottom of the rod string during the downstroke and could be used as an input to sucker rod string design programs and also to evaluate rod string buckling.
2. To predict the stroke rate at which pressures at various locations in the pump would drop below the bubble point pressure of the fluid and evolve gas inside the pump.
3. To indicate areas for improvement in the internal design of sucker rod pumps that would minimize pressure drops through various pump components.

DISCLAIMER

DISCLAIMER

Portions of this document may be illegible in electronic image products. Images are produced from the best available original document.

4. To increase understanding of how pump geometry and pumping rate affect pump filling and contribute to gas interference and gas locking.

The project consisted of four phases: 1) Development of a mathematical flow model, 2) Conducting laboratory flow tests to verify the model, 3) Converting the mathematical model into an easy to use computer program, and 4) Used the model to investigate the effects of viscosity and forces on plunger. Each of these phases is discussed below. Sandia developed the model, conducted the laboratory tests, analyzed the test data, and wrote the computer program. Benny Williams of Harbison-Fischer provided pump design information and engineering guidance. Valuable discussions were also held with Sam Gibbs at Nabla and Dr. Podio at U. of Texas at Austin. TRICO supplied pumps and pump components.

Mathematical Flow Model

There are many ways to model flow in the pump. One method, often used to calculate losses in valves and fittings, is to measure the total pressure drop as a function of velocity in each individual component in the laboratory. That data can then be used to define a loss coefficient for each component, which can then be used to predict losses under other fluid and flow conditions. This method requires that every component of interest be individually tested. In addition, the loss coefficients are not constant over a wide flow range.

Another technique, the finite element method, is often used in flow modeling. But applying finite element modeling correctly to turbulent flow in complicated geometry for flow rates that change throughout the pump stroke requires extensive modeling experience and time consuming mesh generation and iterative solving.

The purpose of this project was to develop a model that is easy to use, allows rapid modification of part geometry, fluid properties, and flow rates and provides easy to understand results. The method selected uses a nodal approach to calculate fluid velocities, pressures, and losses at each change in geometry (or node) along the length of the pump using engineering flow equations. The results are then summed from node to node. The model is based on pipe friction loss and flow equations for single-phase pipe flow from The Crane Co. Technical Paper "Flow of Fluids through Valves, Fittings, and Pipe"[1]. These formulas were supplemented by equations for annular flow in areas such as around the standing and traveling valve balls, past the valve rod, etc [2]. The methodology consisted of 5 steps: 1) dividing the pump into nodes to input the geometry, fluid properties, and flow rate, 2) determine Reynolds number, 3) determine friction factors, 4) determine irreversible friction fluid losses, 5) determine total pressure drop between nodes (see Appendix for details).

Laboratory Testing and Model Verification

The model was first implemented in a large Excel spreadsheet, and focused on the traveling valve. It was not clear at the outset of the project whether the flow equations could be applied to the pump geometry, since they assume long uniform entrance and exit conditions (typically 5-10 pipe diameters) upstream and downstream of the test item, whereas in the actual pump components there are a number of changes in flow area located very closely together. Later testing confirmed that the equations could be applied to typical pump components.

After the model was developed a number of laboratory flow tests were conducted on traveling valves with open and closed cages and various combinations of balls and seats. Sandia does not have an oil pump jack to stroke a sucker rod pump while measuring the flow and pressure drop. Therefore, a test stand was assembled to measure the pressure drop across various pump components under fixed flow conditions. In the tests, water was pumped through the valves at a number of fixed flow rates representative of the range of flow rates encountered during the pumping cycle. API Bulletin 11L3 [3]indicates that a 1 ½" pump may be used over the pump range of 100-600 BPD. This results in a peak flow rate range of 0-55 gpm from the start of the stroke to the middle of the stroke. Test runs with the model were conducted to predict the pressure drops in the traveling valve and throughout the pump for 5-50 gpm in 5 gpm steps. Laboratory tests were then conducted at each of these flow rates. The data from these tests was used to verify and to refine the model.

Adapters were fabricated to provide long straight inlet and outlet conditions for each valve. Digital absolute pressure gauges with an accuracy of 0.01 psi were located approximately 10 diameters upstream and downstream of the test item. The flow rate was adjusted to a number of fixed rates covering the range expected in actual pumping, from zero flow at the beginning of the stroke to the peak flow rate in the middle of the stroke. The flow rate was measured using a magnetic flow meter. The test results were then compared with the pressures predicted by the model. Figure 1 shows the laboratory test setup for individual components.

After completing the modeling and testing of the traveling valve, a number of other components were tested including open and closed cage traveling and standing valves with a variety of balls and seats, high efficiency standing valves, a barrel, plunger, plunger cage, valve rod, upper connector, valve rod guide, and an entire 1 ½" RWAC pump in a seating nipple and tubing. In the case of the entire pump, the hydraulic force on the plunger was measured using a spring balance. The geometry for the entire 1 ½" sucker rod pump and associated hardware was input into the model, including the inlet, standing valve, barrel, traveling valve, plunger, plunger top cage, valve rod, valve rod guide, and tubing. Pressures were calculated at more than 50 locations for a variety of flow rates. Flow tests using the entire pump were then conducted for comparison to the model. In the tests, water was pumped through the sucker rod pump inside of tubing at varying flow rates. Pressure taps were positioned below the standing valve, above the standing valve, above the plunger, and in the tubing above the pump. Figure 2 shows the test setup for the entire pump in tubing. The resulting pressures were then compared to the predictions from the model.

Refinements to the Model

During the initial modeling and testing, the pressure drops observed in the laboratory test and those predicted by the model agreed well at low velocities, but at high flow rates they differed by a factor of 2-3. The model was carefully reviewed and appropriate ranges of the input variables were determined. A sensitivity analysis was performed to determine the relative effect on the predicted pressures introduced by errors in the input pump geometry or fluid properties. The largest potential errors occur from errors in measuring the annular flow area around the ball or in other tight restrictions.

The flow areas of all of the components were carefully measured. Some components contained non-circular flow areas or multiple passages. For example, the flow diameter used for non-circular closed valve cages was modeled by calculating the total flow area of three crescent shaped flow passages added to the circular central flow area, then multiplying by 4, dividing by pi, and taking the square root, to obtain an equivalent diameter. In one of the cages there are three parallel flow passages. This was modeled by setting the flow in each bored hole equal to 1/3 of the total average flow.

It was found that the basic model was correct, but that more nodes were needed to adequately account for all of the significant changes in geometry, such as bevels on the valve seats and seat stop, and the curvature of the valve ball. When these were included, the test data and the modeled data were in excellent agreement.

Visual Basic Program

The pump fluid flow model was converted from the large Excel spreadsheet format into a Visual Basic program which allows easy input of pump geometry, well fluid properties, and flow rate and rapid trade-off studies of the effects of changes in any of these inputs. Figure 3 shows the Visual Basic program user interface. The program also produces predefined output files and plots. The program calculates pressure 'drop' from the inlet of the pump assuming the single-phase incompressible flow using the formulas in the Crane Technical Paper [1]. This includes pressure changes due to gravity head, friction, sudden or gradual expansion or contraction, and Bernoulli effect. Friction factor is determined by iteratively solving the Colebrook formula. Where the pump has more than one channel, the number of channels and the dimensions of an individual channel (the channels are assumed equal) are entered. The velocity is calculated by assuming the flow is split equally between the channels.

The data describing the geometry of the pump is entered as a series of nodes. Hydraulic calculations are made at each node including the effects of the segments between the nodes with results displayed below the end node of a segment. By properly selecting the nodal data, straight segments, sudden expansion / contractions (segments of zero length, but finite area change), or gradual expansion/contractions can be entered. The model uses gradual expansion/contractions to account for chamfers on the ball seat and model the ball, which is round.

The program allows the user to store the nodal data describing a pump or pump part and retrieve the data for later use. Display of the data shows the pressure drops due to head, friction, expansion/contraction, and Bernoulli's effect separately. The program displays two kinds of graphs: a plot of the geometry of the part being analyzed or a plot of the pressure as a function of position. Figure 4 shows the output plot of the traveling valve geometry. Figure 5 shows the pressure drop vs. position for the entire 1.5" diameter pump.

Issues Investigated

Pressure Drop Across Valves

The pressure drop across the standing and traveling valves is important because of the effect it has on pump fillage, gas breakout, and compressive loads on the valve rod. Tests were conducted of the pressure drop across traveling and standing valves over a range from 0-50 gpm.

Various size balls and seats were tested in the valves, as well as open and closed cages. Figure 6 shows the measured and modeled pressure drop through a traveling valve. In one case, there is no ball or seat. In the other case it has a 0.875" ball and a 0.704" ID seat. The modeled data matches the measured data very well for the case with the ball and seat. It matches the case with no ball and seat very well up to 35 gpm, but not as well after that.

In addition to standard valves, two high efficiency standing valves were tested. Figure 7 shows the measured pressure drop through standing valves. The valves included two closed cage valves with different size balls and seats, an insert guided valve, and two high efficiency standing valves. The data shows that using a smaller ball and larger seat ID reduces the pressure drop in closed cage designs, and had approximately the same performance as an open cage design. However, the high efficiency valves had dramatically improved performance compared to the standard valves. The pressure drop through these valves stayed below 1 psi over the full flow range from 0-50 gpm. This is important because it shows that an aerodynamic design that minimizes restrictions and changes in flow area can have a large impact on pressure drop. The same ideas used in the design of these valves could be applied to other pump components.

Figure 8 shows the results of three tests on a standing valve. It is included to show that the test results were very repeatable.

Pressure Drop Across Entire Pump

Figure 9 compares the measured and modeled pressure drop across the standing valve, traveling valve and plunger, pump exit, and the entire pump. These tests were done using the test setup shown in Figure 2, with pressure taps located below the standing valve, above the standing valve, above the plunger in the barrel, and above the pump in the tubing. Several things are worth noting. First of all, there is excellent agreement between the model and the measured values. This is important because it gives confidence in using the model to investigate design tradeoffs and the effect of pumping other viscosity fluids. Another interesting item is that the losses in the traveling valve are higher than those in the standing valve. This would be expected since the flow area in the traveling valve is smaller than in the standing valve. However, the losses in the pump exit (through the top cage past the valve rod) are even higher than in the traveling valve, which was not expected. This shows that use of the model can help to point out areas for improvement in pump design.

Effect of Viscosity

A number of model runs were conducted to determine the effect of pumping different viscosity fluids other than water. Figure 10 shows that over a range of 0.1 cP to 100 cP, and at low to medium flow rates that viscosity change has very little effect on the pressure drop in the valves. At higher flow rates the pressure drop for high viscosity fluids becomes more pronounced. This means that uncertainties in viscosity values downhole will have a small effect on the predicted pressure drops. For example, changing from water at 1 cP to Weeks Island Crude at 15 cP only changed the pressure drop by 6%. Additional testing should be done with a variety of fluids with different viscosities to verify these model results. Laboratory tests by other researchers using fluids with different viscosities and using various valve diameters showed that larger valve flow areas improved the pump efficiency for high viscosity fluids [4].

Effect of Surface Roughness

Machinery handbooks list typical surface roughness for various machining operations, ranging from 1 micro inch for ball bearings to 250 micro inches for rough machined parts. The absolute roughness of a number of the pump parts was measured to determine a range of roughness to use in the friction factor calculations. The absolute roughness ranged from 9 micro inches on the lapped seat to 177 micro inches on the pump inlet. The model was run for a number of fluid viscosities and surface roughness values to see how sensitive the friction factor is to surface roughness. Figure 11 shows the predicted effect of changes in surface finish on the pressure drop in a traveling valve for water. As can be seen, the surface finish has little effect until the absolute roughness exceeds 0.001" (1000 microinches).

Effect of Valve Design Details

Prior researchers have shown the benefits of enlarging the valve seat inside diameter, using open cages rather than closed cages, and increasing the inside diameter of the plunger in order to reduce the forces on the downstroke [5]. All of these modifications reduce fluid restrictions and also reduce the changes in flow area. Several model runs were conducted to perform "what-if" studies on the valve design. Figure 12 shows three model runs of a traveling valve. In case 1, all of the flow area transitions have sharp edges. This gives a pressure loss of 19.6 psi. In case 2, the model is then modified to include the bevel on both sides of the ball seat and at the start of the ball-stop. This reduced the pressure drop to 17.3 psi. In case 3, the flow transitions were smoothed out considerably. This resulted in a pressure drop of 9.8 psi, less than half that of the original case. This points out two things. First, that in order to accurately predict the pressure drop in pump components, the fine details of the components need to be included in the model. Secondly, those fine details are responsible for a significant amount of the pressure drop in the components, and should be carefully evaluated when designing new pump components.

Effect of Ball Chatter

Figure 13 shows tests of the standing valve with the ball and seat, with just the seat, and without the ball or the seat. One of the things that is interesting to note is that with the ball and seat, the pressure drop rises quickly up to a flow rate of approximately 25 gpm. When the flow rate is increased further, the pressure drop decreases rapidly. The model does not predict this. In the flow range from 5-25 gpm the ball was chattering in the valve cage. At 25 gpm the ball stopped chattering and at the same time the pressure drop decreased dramatically. The Crane Technical Paper [1] mentions that check valves should be sized appropriately to fully open, rather than only partially open, in order to minimize losses. This illustrates that there are limitations to what the model can predict.

Forces acting on bottom of sucker rod

Another issue investigated was the load applied to the bottom of the rod string by the hydraulics of the pump. During *upstroke*, it is well recognized that there is a force acting on the bottom of the sucker rod string due to the weight of the fluid being lifted. This force is usually calculated from the pressure difference, ΔP, across the traveling valve:

$$Force = -\pi D_p^2 \Delta P / 4, \qquad (1)$$

where D_p is plunger diameter (see Nomenclature for definition of parameters). There also is a force due to fluid friction drag in the annulus between the plunger and barrel, but this force will

in general be small compared to the weight of the fluid being lifted. Contact between the plunger and barrel can also result in a mechanical friction force. In this discussion the mechanical friction will be ignored. The force on the *upstroke* is tensional and so can not result in buckling.

During *downstroke*, the same effects result in a compressive force acting on the bottom of the plunger. Often, the effect of pressure differential has been ignored during downstroke assuming it is zero since the traveling valve is open. However, tests and model calculations have shown that a pressure difference of up to ~33 psi. or more is required to move fluid from below the traveling valve to above the plunger at peak velocity during the stroke. Therefore, on the downstroke, there is also a force due to the differential pressure, where ΔP is now the pressure across the ends of the plunger. This force needs to be evaluated to determine if it is large enough to contribute to buckling of the rods.

The force of concern is the buckling or effective load [6] not the true load (total load experienced at a molecular level) at the bottom of the rod string. The distinction between buckling and true load can be understood by recognizing that a rod hanging free in a fluid is subject to hydrostatic compression (the molecules are being squeezed), but there is no tendency for the rod to buckle as a result of the hydrostatic load. The buckling load is equal to the true load plus the pressure times area of the rod string, $trueload + PA_r$. The true load at the bottom of the rod string is the pressure below multiplied by the area of the plunger less the pressure above multiplied by the area of the shoulder between the plunger and rods, $P_{below}A_p - P_{above}A_s$ (see Figure 14). If the pressure above times the area of the rod string, $P_{above}A_r$, is added to the true load to get the buckling load, the result is just the pressure differential times the area of the plunger, ΔPA_p since $A_s + A_r = A_p$. Thus, Equation 1 is just the right expression for calculating the buckling load at the bottom of the rod sting when there is no drag or mechanical friction.

The total buckling force at the bottom of the sucker rod string during the downstroke (ignoring mechanical friction) is a result of the combined force due to 1) the pressure differential acting on the ends of the plunger due to resistance to fluid flow through the traveling valve and plunger and 2) the viscous fluid "drag" acting on the sides of the plunger (see Figure 15). The first of these fluid terms is given by Equation 1. The drag is the shear stress on the sides of the plunger wall, τ_W, times the area of the sides of the plunger, $\pi D_p L$, where L is the length of the plunger. Lea and Nickens [7] give the following formula for the force due to shear stress:

$$F_d = -\pi R_i L \frac{\partial P}{\partial z} C_R - \frac{2\pi R_i L \mu}{C_R} V_p \quad , \tag{2}$$

where $\partial P/\partial z = \Delta P/L$. Note: Equation 2 is Lea and Nickens [7] equation with the first term divided by g_C so that the units of both terms of F_d are lbf, not lbm-ft/sec^2. Thus the total buckling force, F, is as a result of adding Equations 1 and 2

$$F = -\pi D_p^2 \Delta P/4 - \pi R_i \frac{(D_b - D_p)}{2} \Delta P - \frac{2\pi D_p L \mu}{(D_b - D_p)} V_p \quad . \tag{3}$$

The $\pi R_i (D_b - D_p)/2$ product is one half the area of the annulus ($\sim \pi D \Delta R/2$ or circumference times thickness) in the parallel plate approximation used by Lea and Nickens [7]. Thus,

$\pi R_i(D_b - D_p)/2$ can be replaced by $\pi(D_b^2 - D_p^2)/8$ (1/2 area of annulus) which results in the following formula for total buckling force:

$$F \approx -\pi \frac{(D_b^2 + D_p^2)}{8} \Delta P - \frac{2\pi D_p L \mu}{(D_b - D_p)} V_p \quad . \tag{4}$$

Equation 4 shows that the total force on the bottom of the rods has two components: 1) a term equal to the pressure differential times the "effective" area of the plunger (area out to approximately half way between the plunger and barrel), and 2) a term proportional to the velocity of the plunger.

Accounting for the shear stress on the sidewalls of the plunger increases the effective area by a factor of $(D_b^2/2 + D_p^2/2)/D_p^2$ or ~ 0.1% for typical 1.5" pump. Thus, the customary approximation of using the area of the plunger when calculating the effect of pressure does not result in a significant error. In discussing the buckling force at the bottom of the sucker rod string, rather than consider the effects of pressure acting on the ends of the plunger and "drag," it is useful to consider the effect of pressure acting on the effective area of the plunger and the effect of plunger velocity. The use of the barrel diameter rather than effective area would be slightly conservative.

As a result of the dynamic behavior of sucker rod pumps, the relationship between peak and average velocity can be complex (Figure 16); however, sinusoidal motion is customarily assumed. For sinusoidal motion, the peak velocity is related to the average velocity according to

$$V_{average} = \frac{V_{peak}}{2\pi}\left(\int_0^{\pi} \sin[\theta] d\theta + \int_{\pi}^{2\pi} 0 d\theta\right) = \frac{V_{peak}}{\pi}. \tag{5}$$

With this relationship it is possible to relate the peak plunger velocity to pump discharge rate:

$$V_p\big|_{peak} = \pi \frac{Q}{A_p} = \frac{Q}{26.7 D_p^2} \frac{\text{ft in}^2\text{day}}{\text{sec bbl}} \quad , \tag{7}$$

where Q is measured in bbl/day. Thus, to produce 600 bbl/day using 1.5" pump, the peak plunger velocity will be $600/26.7 \times 1.5^2 = 10$ ft/sec.

The pressure drop across the traveling valve and plunger can be calculated assuming the empirical equation:

$$\Delta P \approx K Q^2, \tag{8}$$

where the coefficient K has the units psi per $(\text{bbl/day})^2$. Tests of the flow through one type of 1.5" pump traveling valve (.875" ball & .704" seat) show that it takes ~33 psi. to move 55 gal/min (peak sinusoidal flow rate that corresponds to an average pump discharge of ~600 bbl/day) of water through the traveling valve and plunger. This implies a combined traveling valve and plunger coefficient K of ~ 9.3×10^{-5} psi/$(\text{bbl/day})^2$ for a 1 cP fluid.

Substituting Equations 7 and 8 into Equation 4 gives the following equation for the combined buckling force due to pressure and plunger velocity effects:

$$F \approx -\pi \frac{(D_b^2 + D_p^2)}{8} K Q^2 - \frac{2\pi L \mu}{(D_b - D_p)} \frac{Q}{26.7 D_p}, \; ft/s \tag{9}$$

Figure 17 shows the buckling force calculated with Equation 9 using the typical $1^{1/2}$" pump data found in Table 1.

Several experiments were performed in an attempt to verify the physics of Equation (9). First the plunger free fall rate was measured for the pump of Table 1 with the pump full of water and was found to be only 1.2 ft/sec-- significantly less than the 10 ft/sec fall rate required to produce 600 bbl/day without pushing the rod down. A pull rod and a 2' pony rod were attached to the plunger adding weight that should have allowed the plunger to fall faster. Next a 25 lb. weight was added to the pony rod. With this additional weight, the plunger still only dropped at a rate of 2.2 ft/sec. Unfortunately, the experimental set up did not allow the addition of enough weight to exceed the allowable buckling load or have the plunger descend at 10 ft/sec (the peak rate required to produce 600 bbl/day). The relationship between weight and drop rate is nonlinear and there was mechanical friction; hence, it is not appropriate to extrapolate these results to the force require to produce 600 bbl/day. One can, however, conclude from these experiments that to produce this pump at a rate greater than (1.2/10) x 600 = 72 bbl/day the rods must push the plunger down. The pump being used had more mechanical friction than a new pump, but not an excessive amount.

In the second experiment performed to verify Equation 9, the plunger was held in place by a spring balance and the apparent weight of the plunger and associated hardware was measured as a function of flow through the pump. In Figure 18, the measured apparent weight is compared to that expected based on Equation 4 using the measured pressure drop and Equation 9 using the VB program to calculate "*K*." The agreement is very good considering that mechanical friction could not be eliminated from the test and caused erratic behavior. The point where the apparent weight went to zero (~35 gal/min corresponding to 380 bbl/day) just happened to be the limit of the plumbing delivering water to the pump. At this flow rate the plunger floated up and weight would have been required to keep it in position.

The pressure profiles measured and modeled under these fixed flow conditions can be used to predict the time varying compressive load applied by the pump hydraulics to the valve rod.

Figure 17 shows that when the pump produces 600 bbl/day of a 1 cP fluid, the hydraulics of the pump result in a buckling force of ~65 lbf which happens to be the same as the load, reported by Lea and Nickens [7], required to buckle a 7/8" sucker rod. Note, that only increasing the viscosity to 10 cP is required to increase the buckling load to ~150% of that required to buckle the rod. Thus one concludes that pump hydraulics can be a significant factor in whether the bottom sucker rods buckle. Figure 19 shows that changing the clearance between the plunger and barrel can significantly reduce the buckling load at higher viscosities.

Follow-On Work

This project developed a significant tool for predicting the effects of various changes in pump design and operation on pressure drops and fluid drag loads in a sucker rod pump. Sandia is planning to make this program available to the industry in a user-friendly PC based computer program. Sandia plans to extend this work by testing a full size, transparent, instrumented pump in the laboratory using various viscosity fluids and stroke rates. These tests will be done at the University of Texas at Austin, followed by testing a highly instrumented pump downhole.

Recommendations for future work include testing valve components using fluids with different viscosities, measuring pressures in the pump and the force on the plunger while stroking the pump, extending the model to include multi-phase flow, partial pump fillage, table lookup to input pump component geometry, input of the pump velocity directly from dynamometer data, and adding the correlations to convert from uphole to downhole viscosity and density.

Conclusions

1. An engineering single phase model was developed for analyzing flow in sucker rod pumps. The model results were verified by laboratory testing, and agree closely with the laboratory data. The model has been implemented in a visual basic program for easy input and output.
2. The model predicts that:
   a) For low viscosity fluid, pressure drop due to surface roughness is low for absolute roughness <0.01".
   b) Pressure losses due to viscosity are low for viscosities below 100 cP.
   c) Most of the pressure drop in a pump is in the valves, connectors, and rod guide, and can be reduced by minimizing restrictions and abrupt changes in flow area.
   d) The differential pressure across the traveling valve and plunger on the downstroke can become significant. At high stroke rates they can put the valve rod in compression.
   e) The fine details of both the model and of the hardware are important. Refining the geometry improves the accuracy of the model.

References

1) Flow of Fluids Through Valves, Fittings, and Pipe, Crane Technical Paper No. 410, Joliet, IL., 1991.

2) Reed, T.D.; and Pilehvari, A.A.: A New Model for Laminar, Transitional, and Turbulent Flow of Drilling Muds, SPE 25456, Production Operations Symposium, Oklahoma City OK, 1993.

3) API Bulletin 11L3 Bulletin on Sucker Rod Pumping System Design Book

4) Yu Guoían, Ji Jiachang, Xu Yuangang, Zhao Laijun Ban Shengli, Liang Shujuan: "Indoor Experiments on the Effects of Viscosity, Valve Diameter and Stroke Rate on Pump Efficiency in a Sucker Rod Pumping System" , Journal of Xiían Petroleum Institute, Vol. 11, No. 4, July 1996

5) Allen, L.F. and Svinos, J.G.: Rod Pumping Optimization Program Reduces Equipment Failures and Operating Costs, SPE 13247.

6) Lea, J.F.; and Pattillo, P.D.: Interpretation of Calculated Forces on Sucker Rods, SPE 25416.

7) Lea, J.F, and Nickens, H.V.: Beam Lift Issues, Appendix, Southwestern Petroleum Short Course, Lubbock TX, 1998.

Acknowledgments

The authors gratefully acknowledge the support of Benny Williams of Harbison Fischer (Formerly at TRICO) for providing pump design information, engineering and technical support, sucker rod pump design information and information on in-house testing, TRICO for supplying the pump and pump components, Sam Gibbs of Nabla for discussions on the modeling effort, Jimmie J. Westmoreland at Sandia for assistance in the laboratory testing, and Charles E. Hickox Jr. at Sandia for guidance in the modeling. This work was supported by the United States Department of Energy under Contract DE-AC04-94AL85000. Sandia is a multiprogram laboratory operated by Sandia Corporation, a Lockheed Martin Company, for the United States Department of Energy.

Table 1: Typical Data for a $1^{1/2}$" Pump

Barrel diameter (D_b)	1.5 in
Plunger diameter (D_p)	1.498 in
Plunger length (L)	3 ft
Fluid viscosity (μ)	1→500cp
Empirical pressure coefficient (K)	~ $9.3\text{x}10^{-5}$ → ~$1.6\text{x}10^{-4}$ psi./(bbl/day)^2
Pump average discharge rate (Q)	→ 600 bbl/day

Nomenclature:

A_p = Area of plunger,

A_s = Area of shoulder between plunger and rod string,

A_r = Area of rod string,

C_R = Radial clearance, = $(D_b - D_p)/2$,

cP = Centipoise = lbf-s/(ft^2 47869),

D_b = Barrel diameter,

D_p = Plunger diameter,

F = Total buckling force,

F_d = Drag force,

g_c = 32.17 lbm-ft/lbf-s^2,

K = Empirical pressure coefficient (psi/(bbl/day)^2),

L = Length of the plunger,

P = Pressure,

P_{above} = Pressure above,

P_{below} = Pressure below,

ΔP = Pressure difference across the plunger,

Q = Pump discharge (bbl/day),

R_i = Wall corresponding to inner wall of the plunger/barrel gap,

V_p = Plunger velocity,

V_{peak} = Peak velocity,

$V_{average}$ = Average velocity,
z = Vertical coordinate,
μ = Fluid viscosity at the pump,
θ = Time coordinate, and
τ_w = Shear stress at plunger wall.

Appendix

The method consists of the following 5 steps (notation taken from the Crane Technical Paper [1]):

1) Divide the pump into logical nodes at each change in geometry. Input the following parameters into the model for each node:

Pump geometry:		Units	
$d_{i,o}$	inside and outside flow diameters	inches	measured
z	length between nodes	inches	measured
ε	surface roughness	inch	measured, or approximate per Crane p.A-23
N	number of flow channels		

Fluid properties:			
ρ	density	lbm/ft^3	Crane p.A-6 (62.4 lbm/ft^3 for water at 50 F)
μ	viscosity	cP	Crane p. A-3 (1.05 cP for water at 60 F)

Flow conditions:

Fixed flow rates are used to compare to lab tests, sinusoidal or variable cycle flow rates to compare to pumping. The model uses the average instantaneous flow rate through the pump to calculate the velocity at each node.

q	flow rate	gpm	
$v = \frac{183.3 * q}{d^2}$		ft/sec	for straight pipe flow
$v = \frac{183.3 * q}{d_o^{\,2} - d_i^{\,2}}$		ft/sec	for annular flow

2) Determine Reynolds number at each node for each flow rate:

$$\mathrm{Re} = \frac{123.9 d v \rho}{\mu}$$

Where d= Pipe ID for straight pipe

$d = d_{Equivalent} = d^2_{Lamb}/d_{Hydraulic}$ for Annular Flow (see Reed [2] for definition of Lamb and Hydraulic diameter).

$$d_{Equivalent} = \frac{\left[d_o^{\,2} + d_i^{\,2} - ((d_o^{\,2} - d_i^{\,2}) / \ln(d_o / d_i))\right]}{(d_o - d_i)}$$

3) Determine the Friction Factor at each node for each flow rate. Use the Colebrook equation, solving iteratively, to determine $f_{Fanning}$. f_{Moody} is then 4 x $f_{Fanning}$. For straight pipes, d = pipe ID. For annulus, d = $d_{Equivalent}$, NOT $d_{Hydraulic}$.

$$f_{Fanning} = \frac{1}{\left[4 * \log\left[\frac{d_{Equivalent}}{\varepsilon}\right] + 2.28 - 4\log\left(1 + \frac{4.67\left(\frac{d_{Equivalent}}{\varepsilon}\right)}{\mathrm{Re}\sqrt{f_{Fanning}}}\right)\right]^2}$$

$$f_{Moody} = \frac{64}{\mathrm{Re}} \quad \text{for Re<2100}$$

$$f_{Moody} = 4 * f_{Fanning} \quad \text{for Re>2100}$$

Using an initial guess of f = 0.005, solve iteratively.

4) Find total irreversible fluid friction losses between each node.

$$\Delta P = \frac{0.001294 f_{Moody}\left(\frac{z}{12}\right)\rho v^2}{d}$$

Where d = d_{ID} pipe for straight pipe flow
d = $d_{Hydraulic}$ for annular flow

$$\Delta P = \frac{\rho K v^2}{144 * 2g}$$

Where K is given in Crane A-26 through A-29 for expansions, contractions, entrances, exits. Use the local K and v values as appropriate for the smaller or larger pipe. The angle Θ is the total included angle, not the half angle. Add together the ΔP due to straight pipe friction and the ΔP due to changes in diameter.

$$K_2 = \frac{0.8\left(\sin\frac{\Theta}{2}\right)(1 - \beta^2)}{\beta^4}$$

For sudden or gradual contraction, Θ≤45°

$$K_2 = \frac{0.5\left(1-\beta^2\right)\sqrt{\sin\left(\frac{\Theta}{2}\right)}}{\beta^4}$$ For sudden or gradual contraction, Θ>45°

$$K_2 = \frac{2.6\left(\sin\frac{\Theta}{2}\right)\left(1-\beta^2\right)^2}{\beta^4}$$ For sudden or gradual enlargement, $\Theta \leq 45°$

$$K_2 = \frac{\left(1-\beta^2\right)^2}{\beta^4}$$ For sudden or gradual enlargement, Θ>45°

5) Determine the total pressure drop between each set of nodes using Bernoulli's equation to account for changes in elevation, flow velocity, and irreversible friction losses.

$$P_1 - P_2 = \frac{\rho}{144}\left((z_2 - z_1) + \frac{v_2^{\,2} - v_1^{\,2}}{2g}\right) + \Delta P_{FrictionTotal}$$

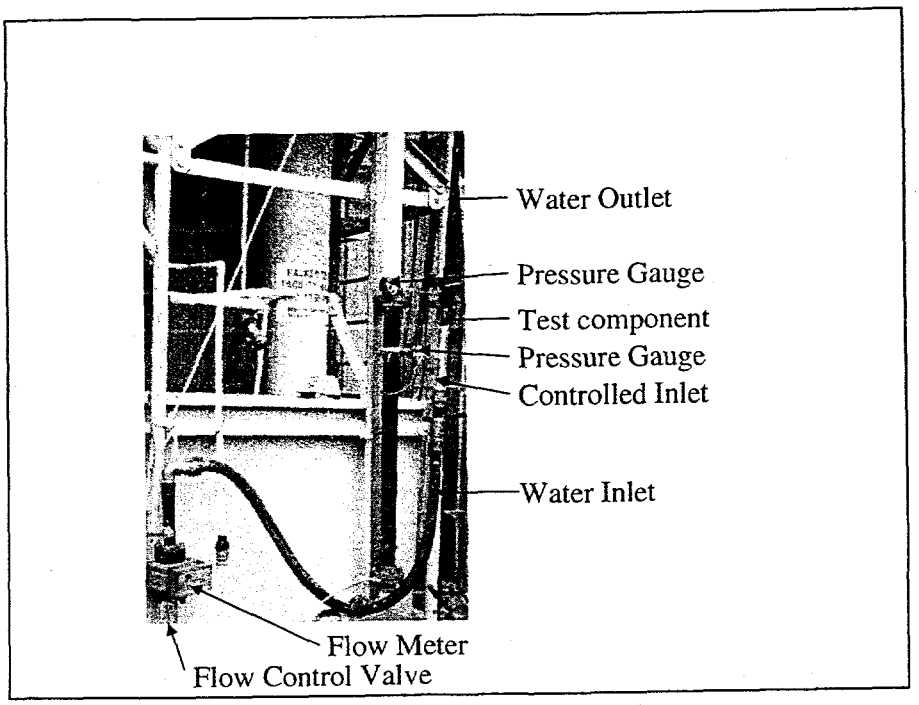

Figure 1: Laboratory Test Set-Up for Individual Components

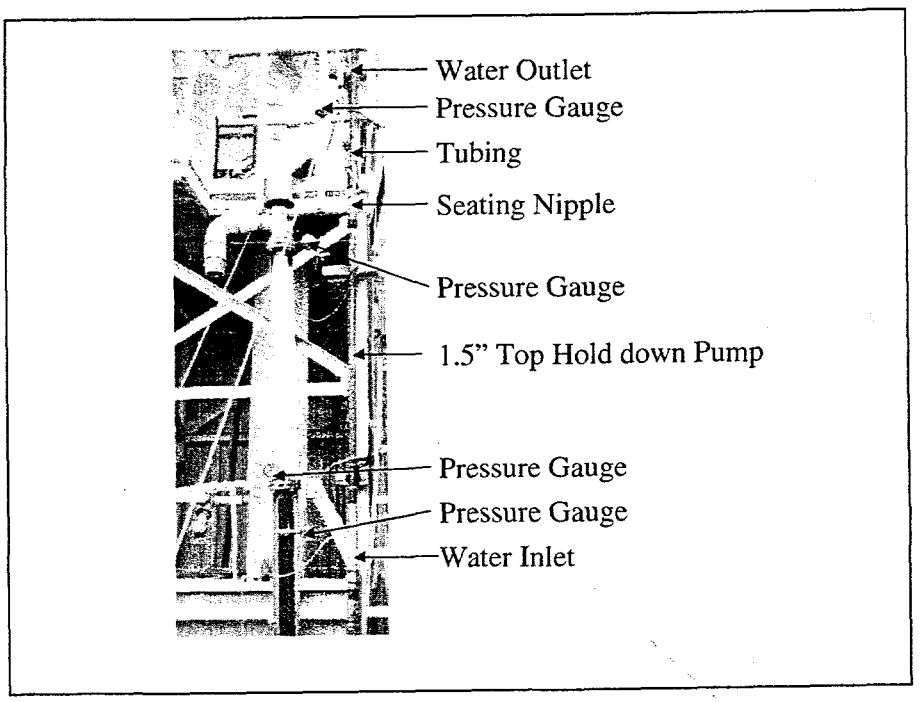

Figure 2: Laboratory Test Set-Up for Complete Pump

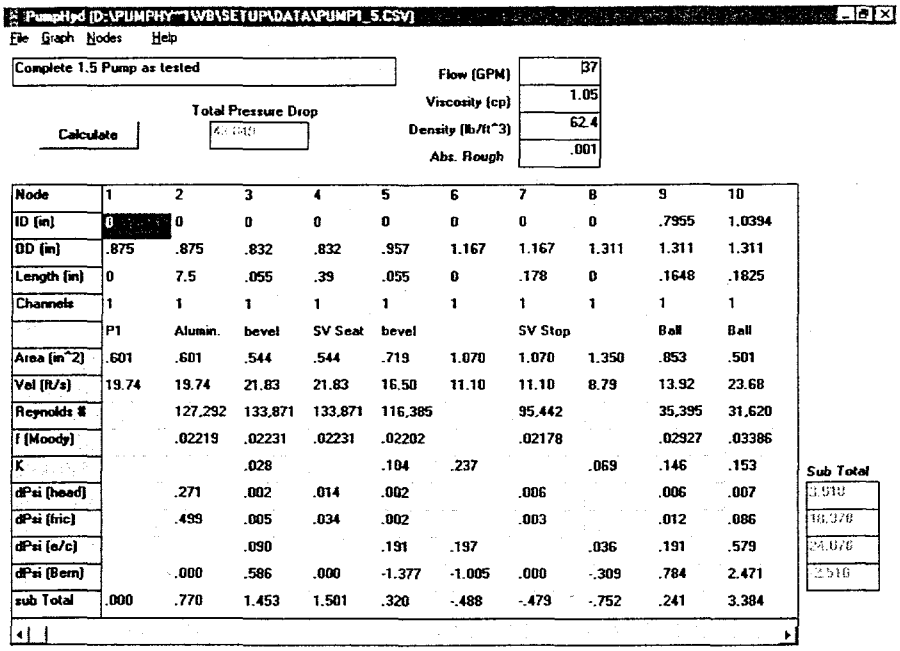

Figure 3: Visual Basic Program User Interface.

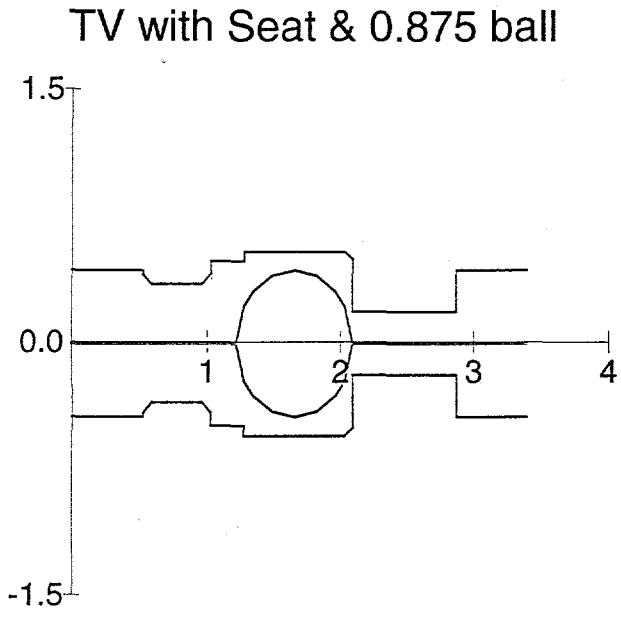

Figure 4: Visual Basic Program Display of Traveling Valve Geometry. Vertical axis is diameter and horizontal axis is length.

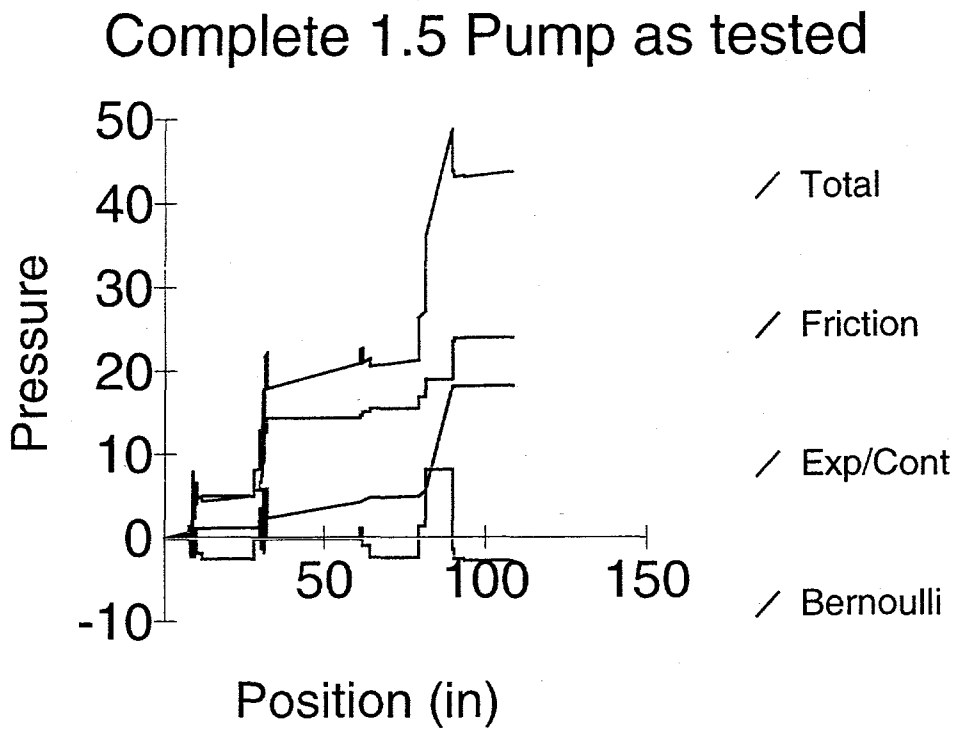

Figure 5: Visual Basic Program Display of Pressure Drops as a Function of Position

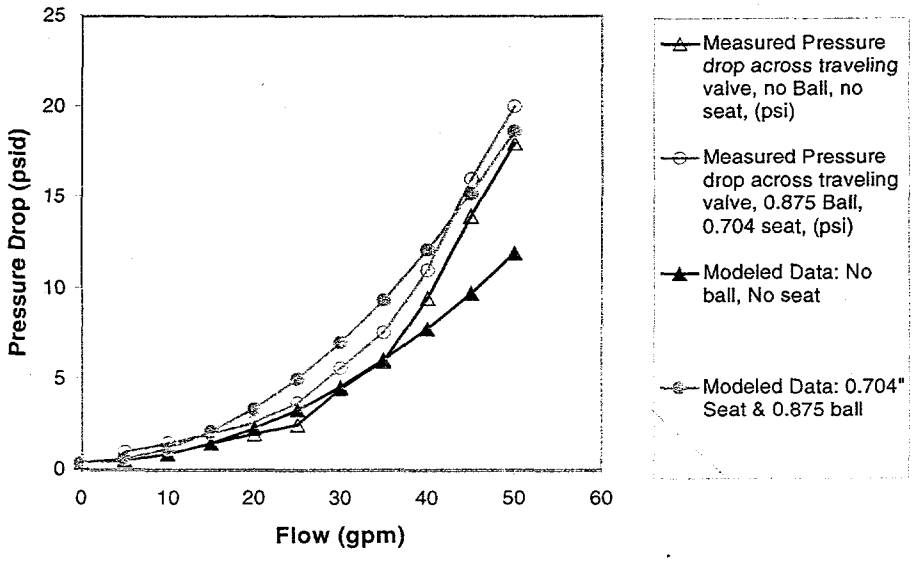

Figure 6: Modeled and Measured Pressure Drop in Traveling Valve

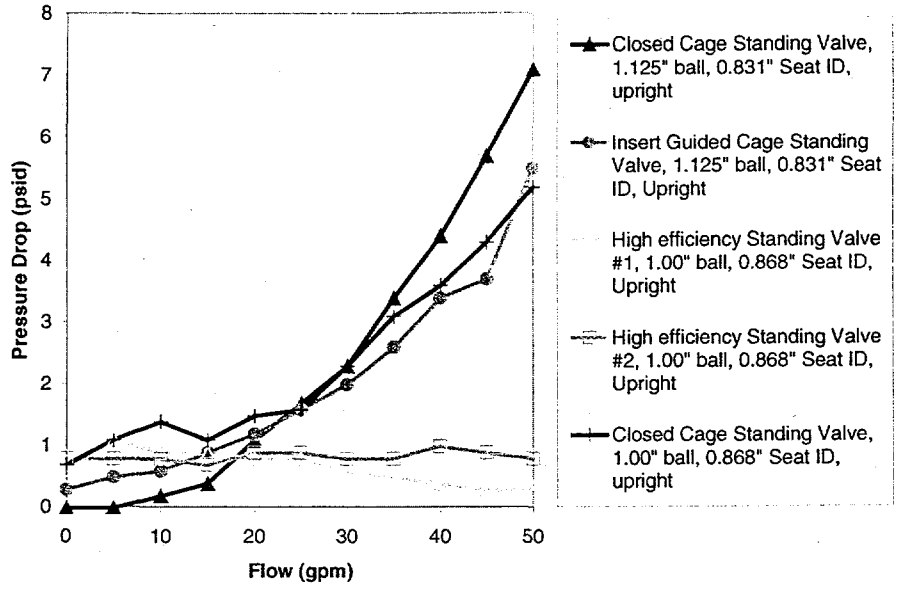

Figure 7: Measured Pressure Drop vs. Flow Rate for Standing Valves

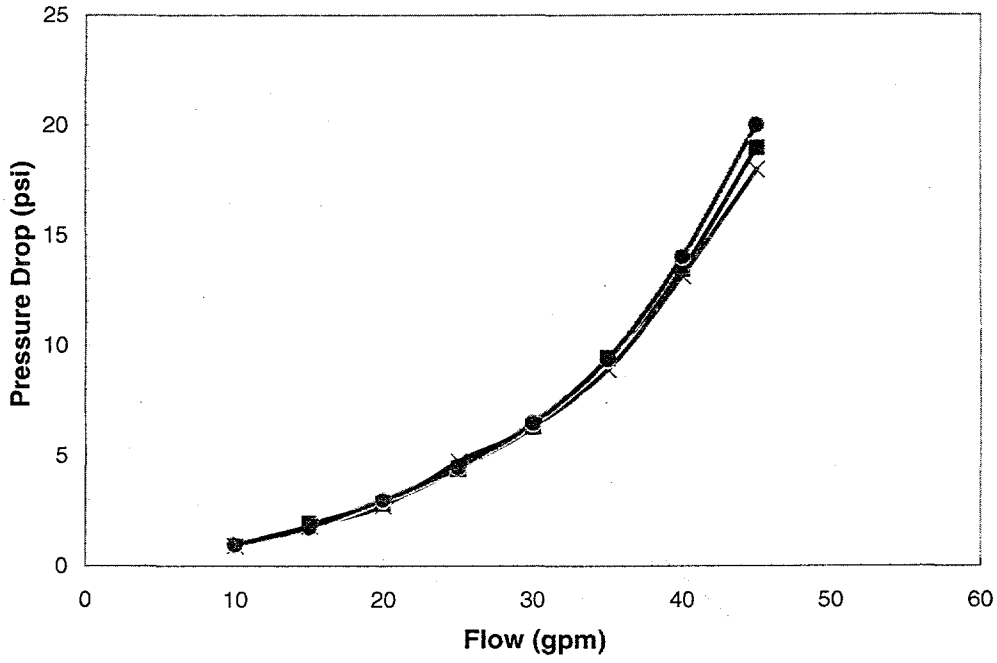

Figure 8: Repeatability of Pressure Drop vs. Flow Rate Test of Standing Valve

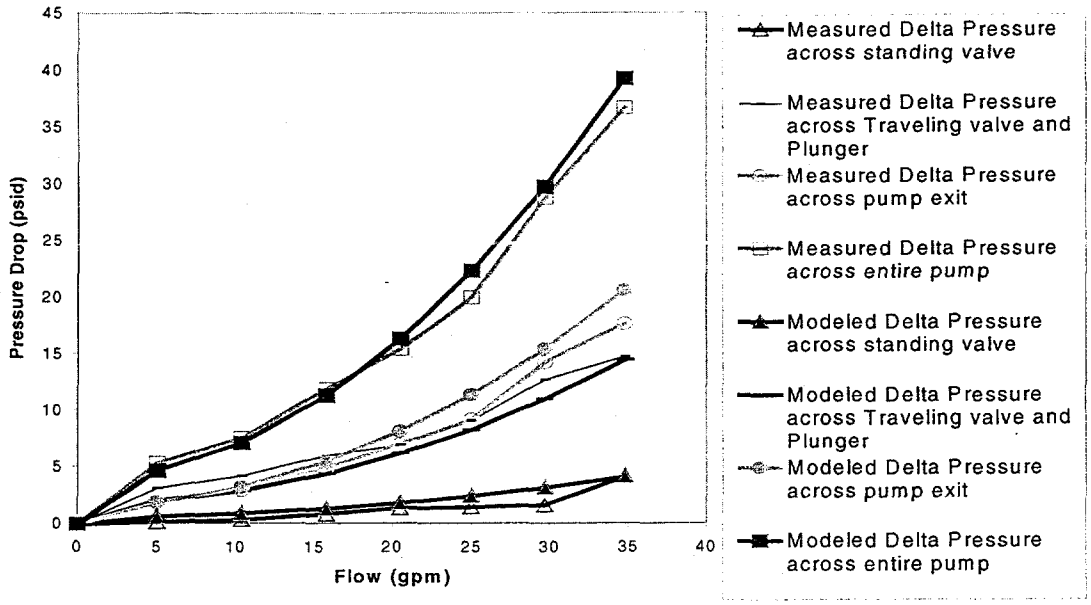

Figure 9: Modeled and Measured Pressure Drop vs. Flow Rate in 1.5" Pump

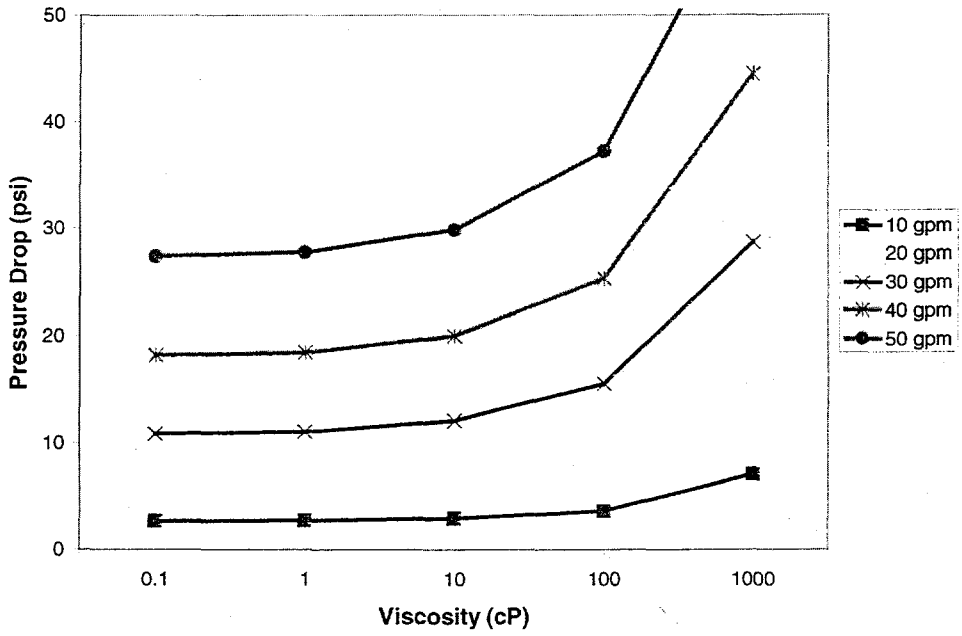

Figure 10: Modeled Effect of Viscosity on Pressure Drop, 1.5" Traveling Valve

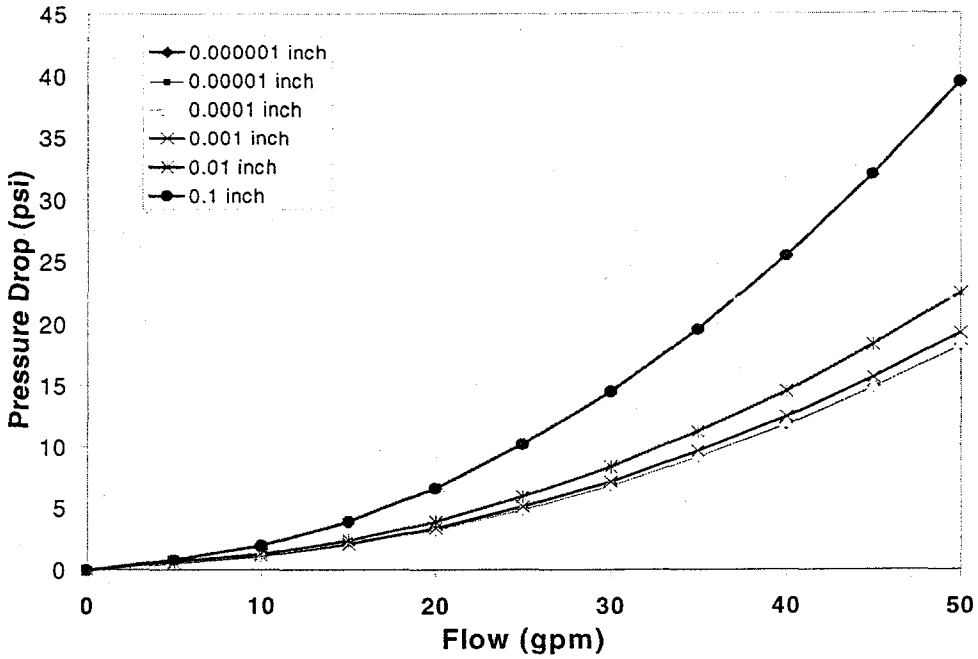

Figure 11: Modeled Effect of Absolute Surface Roughness in Traveling Valve for Water

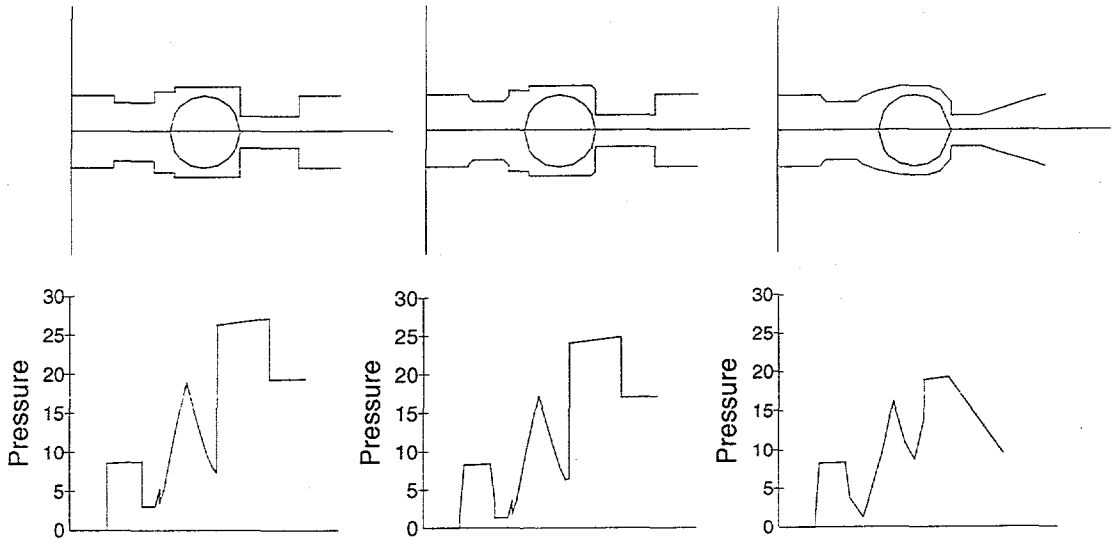

Case 1
No Bevels
Pressure Drop 19.6 psi

Case 2
Beveled Seat, Stop
Pressure Drop 17.3 psi

Case 3
Beveled Seat, Stop,
Smooth Transitions
Pressure Drop 9.8 psi

Figure 12: Example of Importance of Model and Hardware Details for Traveling Valve (top geometry, bottom pressure drop)

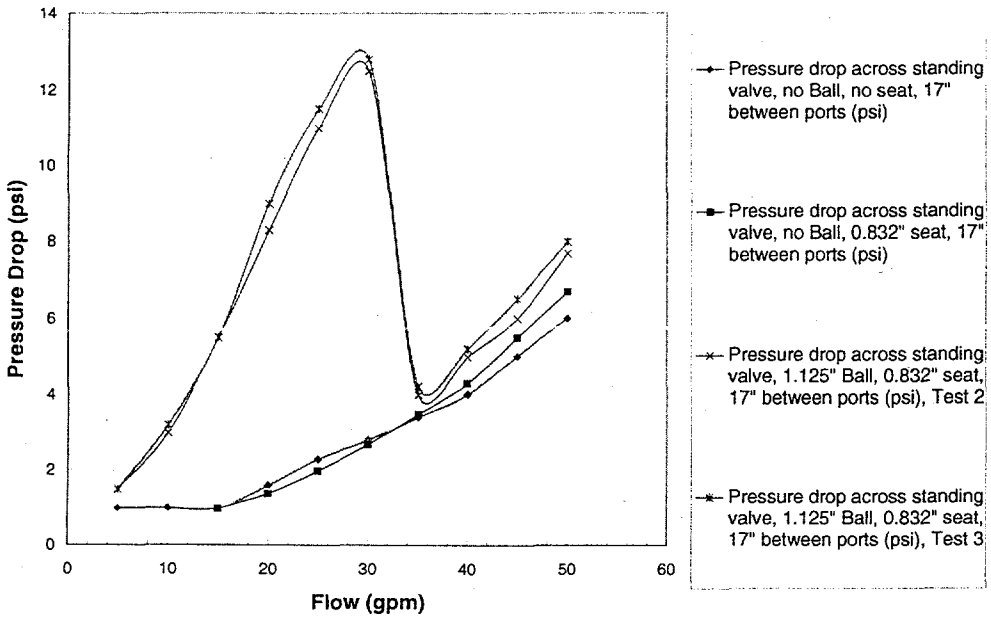

Figure 13: Pressure Drop in Standing Valve With Ball vs. Without Ball

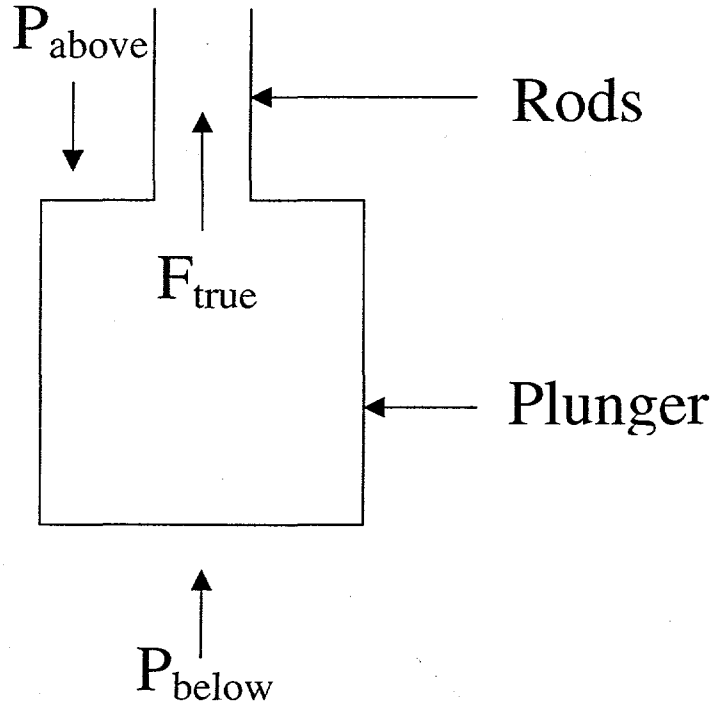

Figure 14 : Relationship Between Pressure Above and Below and True Force

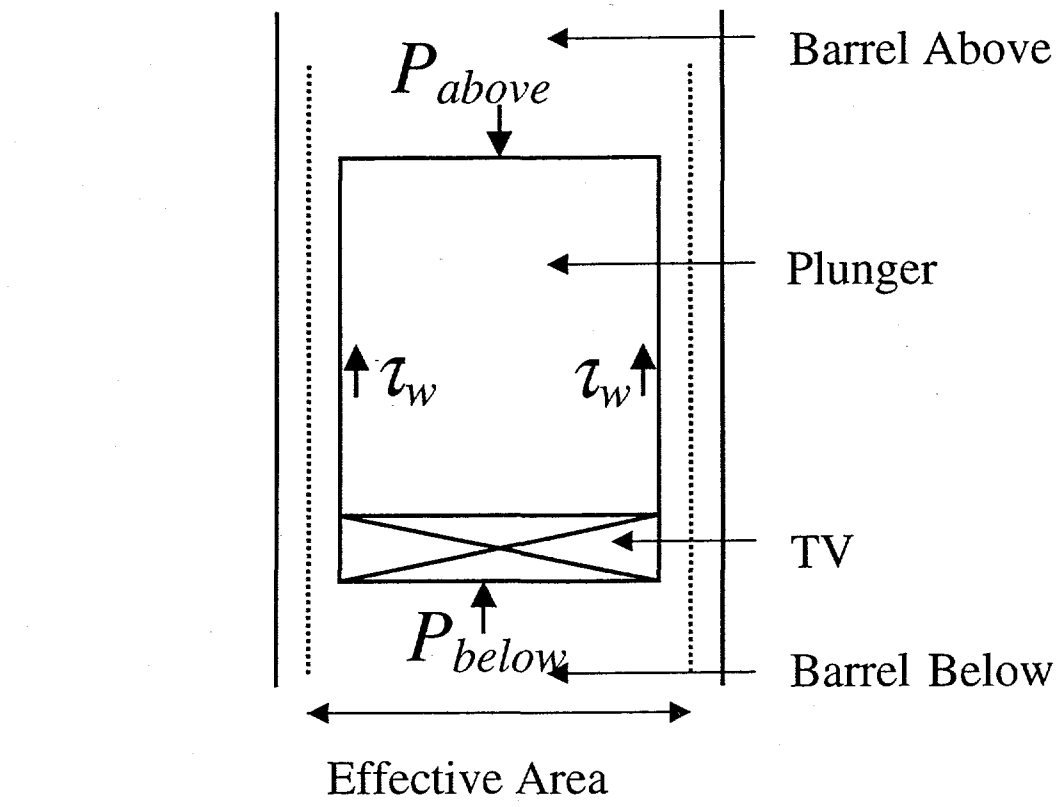

Figure 15: Plunger Drag Forces

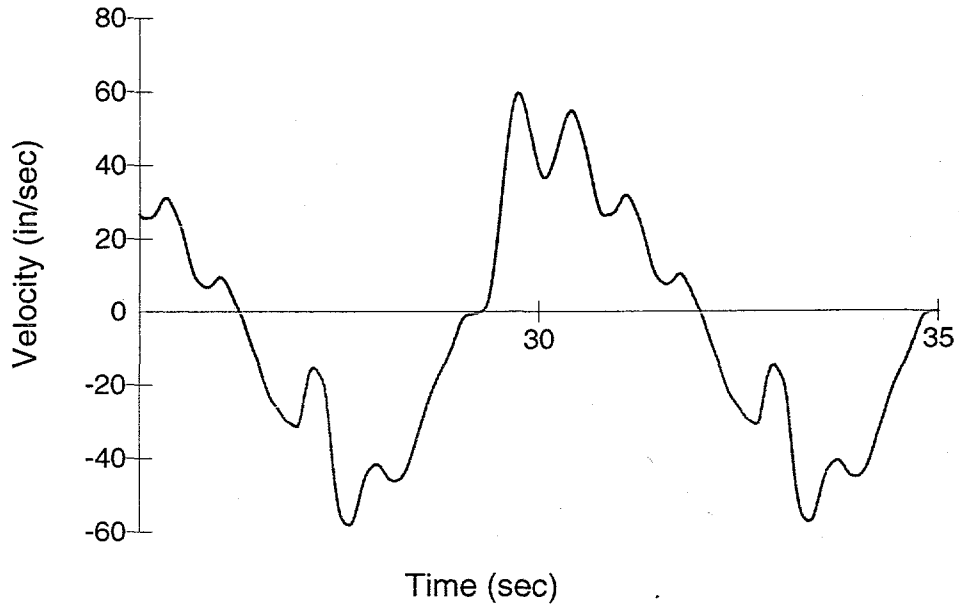

Figure 16: Plunger Velocity Measured at the Pump

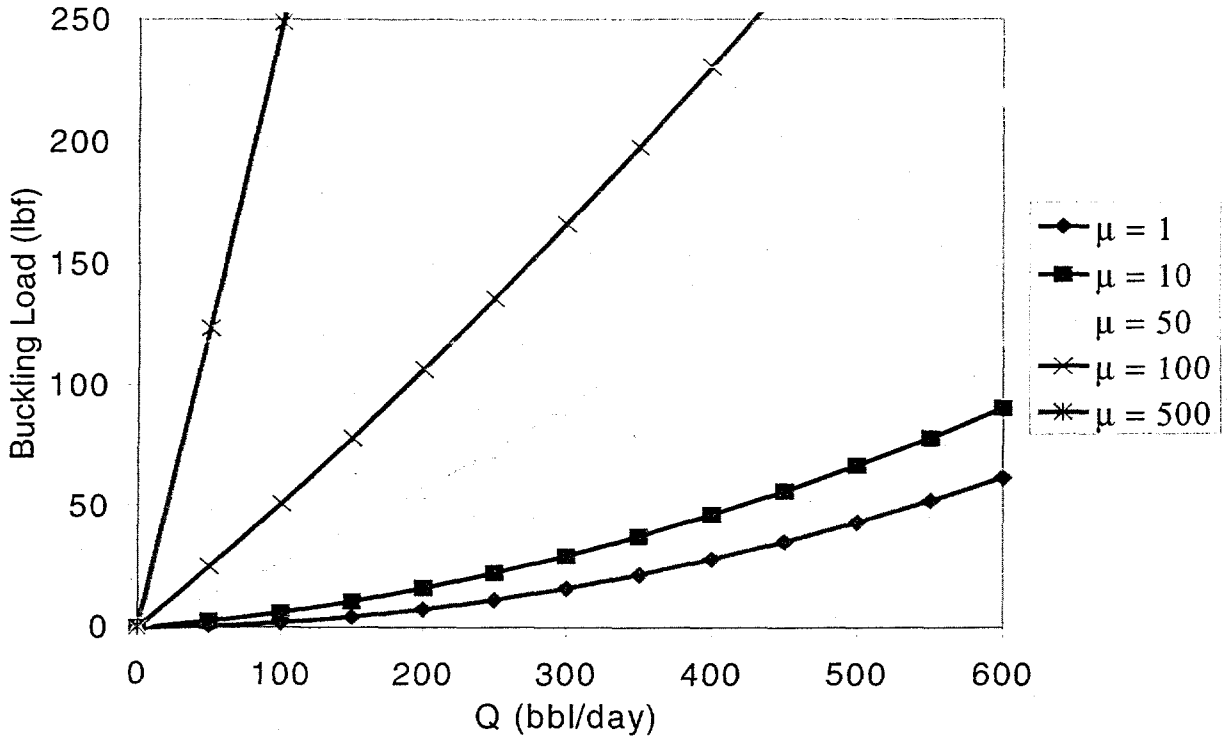

Figure 17: Buckling Force as a Function of Pump Discharge Rate using data in Table 1

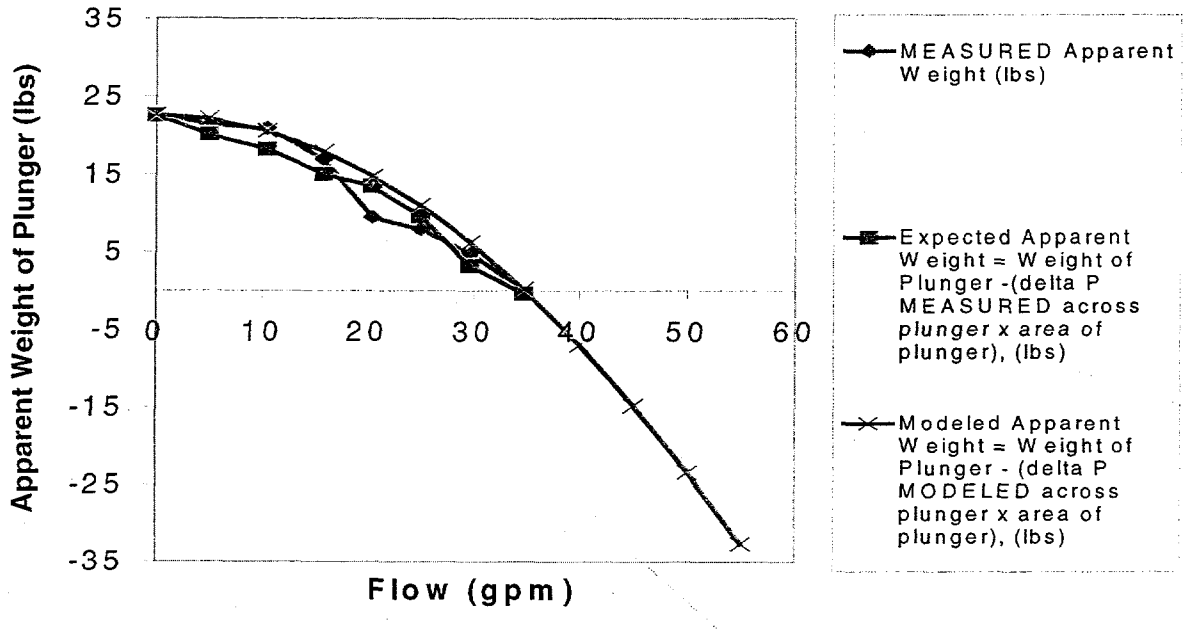

Figure 18: Apparent weight of Plunger as a Function of Flow through Pump

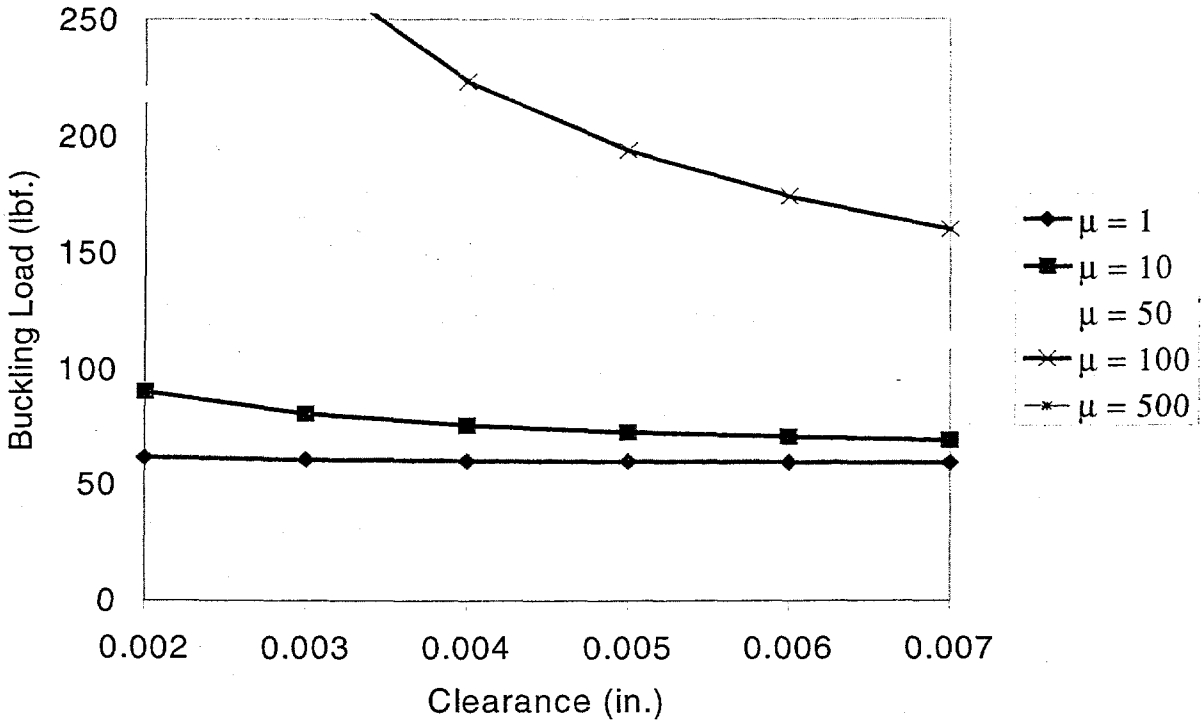

Figure 19: Buckling load as a function of clearance for 600 bbl/day (note the 500 cP curve is off the scale).